European Review for Medical and Pharmacological Sciences 2020; 24: 4190-4202

Circ_0056618 promoted cell proliferation, migration and angiogenesis through sponging with miR-206 and upregulating CXCR4 and VEGF-A in colorectal cancer

X. ZHENG[1], Y.-F. MA[2], X.-R. ZHANG[1], Y. LI[1], H.-H. ZHAO[1], S.-G. HAN[1]

[1]Nuclear Medicine Laboratory, Tangshan People's Hospital, Lunan District, Tangshan City, Hebei Province, China
[2]Radiology Department, the Second Affiliated Hospital of Suzhou University, Suzhou City, Jiangsu Province, China

Abstract. – OBJECTIVE: Growing evidence has revealed that circular RNAs (circRNAs) play important roles in the development of cancers, including colorectal cancer (CRC). In this study, we mainly focused on the expression of circ_0056618 and potential functions of circ_0056618 in CRC patients.

PATIENTS AND METHODS: RT-PCR was performed to detect circ_0056618 and miR-206 expressions in CRC tissues and adjacent non-tumor tissues. Correlation analysis was used to analyze the correlation between circ_0056618 and miR-206. Kaplan-Meier method was conducted to analyze the overall survival (OS) for CRC patients. Moreover, CCK-8 assay was used to measure cell proliferation ability and transwell assay was performed to detect cell migration ability. Besides, tube formation assay was performed to measure cell angiogenesis capacity. Western blot (WB) was performed to measure protein levels of tissues samples and CRC cell lines. Notably, the Luciferase reporter assay was performed to prove the binding sites in circ_0056618 with miR-206, miR-206 with CXCR4 and VEGF-A.

RESULTS: We found that circ_0056618 was elevated in CRC tumor tissues and CRC cell lines, which was related to poor diagnosis for CRC patients. MiR-206 was reduced in CRC tissues, which was negatively related with circ_0056618. Protein levels of CXCR4 and VEGF-A were elevated in CRC tumor tissues, which were negatively related with miR-206. Circ_0056618 inhibition inhibited proliferation, angiogenesis and migration of HT29 cells, and repressed protein levels of Cyclin D1, VEGF-A and N-cadherin and increased E-cadherin. Notably, Luciferase reporter assay indicated that circ_0056618 could sponge with miR-206, which could directly target at CXCR4 and VEGF-A. Finally, we proved a pathway that circ_0056618 promoted cell proliferation, migration and angiogenesis through sponging with miR-206 and removing the repressing effects of miR-206, thereby upregulating CXCR4 and VEGF-A in CRC.

CONCLUSIONS: Above all, this study revealed that circ_0056618 was increased in CRC tissues, which was related with the poor OS of CRC patients. We found that circ_0056618 could promote cell proliferation, migration and angiogenesis through sponging with miR-206 and upregulating CXCR4 and VEGF-A in CRC, which might provide a novel potential therapeutic target for treating CRC.

Key Words:
Circ_0056618, MiR-206, CXCR4, VEGF-A, Angiogenesis, Colorectal cancer.

Introduction

Colorectal cancer (CRC) is one of the most commonly digestive system cancers. Its incidence and mortality are among top five in the world and it has been reported to be the second cause of cancer death worldwide[1-4]. Although therapeutic treatments and diagnosis methods have increased diagnosis rate and 5-year survival rate for CRC patients; however, the prognosis of patients with metastasis and distant metastasis is extremely poor[5-8]. Therefore, new drugs with selective cytotoxicity and early-stage diagnosis methods for CRC patients are urgently needed. CircRNAs play important functions in the progression of CRC[9-15], which shape a closed loop structure that has no terminal 5' caps and 3' polyadenylated tails[16-22]. CircRNAs can regulate various functions through sponging with microRNAs (miRNAs), thereby regulating gene expressions, which is called a competing endogenous RNA (ceRNA) mechanism[16-22]. Consistently, Li et al[10] demonstrated that circRNA CBL.11 suppressed cell proliferation

Corresponding Author: Han Sugui, MD; e-mail: hansugui2006@sina.com

through sponging with miR-6778-5p in colorectal cancer. Wang et al[13] found that exosome-delivered hsa_circ_0005963 could promote glycolysis to induce chemoresistance via miR-122/PKM2 axis in colorectal cancer. Although researchers have found some roles of circRNAs in CRC, however, most circRNAs and the functions in CRC are largely unknown. Circ_0056618 was a novel circRNA reported to be elevated in gastric cancer and it regulated cell proliferation and metastasis through regulating CXCR4 in gastric cancer[23]. However, expressions of circ_0056618 and its role in CRC remained unknown.

MicroRNAs (miRNAs) can affect various functions by binding to the 3' untranslated regions (UTR) of target genes in CRC [24-27]. MiR-206 is a miRNA that can regulate invasion, proliferation and angiogenesis in cancers[28-33], such as non-small cell lung cancer[33], prostate cancer[30], breast cancer[32], etc. Zhu et al[28] demonstrated that miR-206 was significantly repressed in CRC and it was involved in regulating CRC cell proliferation and metastasis. However, the detailed mechanism of miR-206 in CRC remained not fully understood.

In this study, we investigated the expressions of circ_0056618 in CRC tumor tissues and non-tumor tissues, founding that it was elevated in CRC tissues and CRC cell lines. As a result, we aimed at exploring the functions and potential mechanism of circ_0056618 in CRC patients.

Patients and Methods

Tissues Samples

60 cases of CRC patients with tumor tissues and the corresponding non-tumor tissues were collected after surgical resection in our hospital from September 2012 to October 2013, which were frozen at -80°C. Detailed clinical parameters of CRC patients were showed in Table I. All patients signed the informed consent and this study was approved by Faculty of Medicine's Ethics Committee of our hospital.

Cell Culture

Human colon epithelial cell line NCM460 (INCELL, San Antonio, TX, USA) and human CRC cell lines, including LoVo, HCT116, SW480, SW620 and HT29 (ATCC, Manassas, VA, USA), were cultured in Dulbecco's Modified Eagle's Medium (DMEM; Invitrogen, Carlsbad, CA, USA), which were supplemented with 10% fetal bovine serum (FBS; Gibco, Grand Island, NY, USA), 1% penicillin (HyClone, South Logan, UT, USA) and streptomycin (HyClone, South Logan, UT, USA). Cells were cultured in an incubator with 37°C and 5% CO_2.

Construction of SiRNA and Cell Transfection

Small interfering RNA (siRNA) for circ_0056618 was constructed into a plasmid, which was named si-circ_0056618. SiRNA negative control (si-NC) was obtained from Invitrogen (Carlsbad, CA, USA). Cells were seeded on 6-well plates until they reached about 60% confluence. Then, si-circ_0056618 or si-NC was respectively transfected to prepared cells with Lipofectamine 2000 (Invitrogen, Carlsbad, CA, USA) according to its protocol. Cells with circ_0056618 down-regulation were obtained. After MiRNA transfection, cells were seeded on 6-well plates until they reached about 60%. Then, miR-206 inhibitor or inhibitor NC was respectively transfected into prepared cells with Lipofectamine 2000 according to the protocol.

RNA Extraction and Quantitative Real-Time PCR

Total RNAs in tissue samples and cell lines were extracted by TRIzol reagent (Invitrogen, Carlsbad, CA, USA) according to its protocol. RNAs were reversed transcribed into cDNA by PrimeScript™ RT reagent Kit (TaKaRa, Dalian, China) in accordance with its protocol. PCR primers were synthesized by Gene Pharma (Gene Pharma, Shanghai, China), which were listed in Table II. The mRNA expressions were detected by SYBR Premix Ex Taq II (Takara, Dalian, China), relative gene expressions were calculated by $2^{-\Delta\Delta CT}$ method and were normalized to β-actin or U6.

Protein Extraction and Western Blot

Total proteins of human tissue samples and CRC cell lines were extracted using a radioimmunoprecipitation assay buffer (RIPA) protein extraction buffer (Sigma-Aldrich, St. Louis, MO, USA) with a protease inhibitor (Roche, Basel, Switzerland) and the concentrations were detected using a bicinchoninic acid (BCA) kit (Pierce Chemical Co., Rockford, IL, USA). 40 μg total proteins form each group were added onto 10% sodium dodecyl sulphate-polyacrylamide gel electrophoresis (SDS-PAGE) for separation and

Table I. Correlation between circ_0056618 expression and clinicopathological features in patients of CRC.

Parameters	Total (n=60)	Low circ_0056618 (n=30)	High circ_0056618 (n=30)	*p*-value
Age				0.793
<65 Y	36	17	19	
≥65 Y	24	13	11	
Gender				0.596
Male	37	20	17	
Female	23	10	13	
Tumor site				0.604
Colon	33	15	18	
Rectum	27	15	12	
Tumor size				
<5 cm	27	18	9	0.037*
≥5 cm	33	12	21	
TNM stage				
I-II	31	20	11	0.038*
III-IV	29	10	19	
Lymph node metastasis				
Yes	26	8	18	0.018*
No	34	22	12	
Distant metastasis				
Yes	21	6	15	0.029*
No	39	24	15	

were transferred onto polyvinylidene difluoride (PVDF) membranes. Membranes were blocked with non-fatty milk at room temperature for 1 h and washed with Tris Buffered Saline and Tween (TBST; Boster, China) for three times. Primary antibodies were used to incubate these membranes, which were purchased from Abcam (Abcam, Cambridge, MA, USA): CXCR4 (ab1670, 1:500, 39 kDa), VEGF-A (ab46154, 1:5000, 23 kDa), Cyclin D1 (ab134175, 1:5000, 34 kDa), N-cadherin (ab18203, 1:1000, 100 kDa), E-cadherin (ab40772, 1:10000, 110 kDa) and β-actin (ab8226, 1:5000, 42 kDa). After incubating overnight at 4°C, membranes were then incubated with corresponding secondary antibodies (1:5000) for 1 h. Finally, proteins were visualized by adding SuperSignal® ECL Kit (Thermo Fisher Scientific, Waltham, MA, USA) in enhanced chemiluminescence (ECL) detection system (Thermo Fisher Scientific, Waltham, MA, USA).

Cell Viability Assay

Cell viability was tested by using Cell Counting Kit-8 (CCK-8) assay (Dojindo Molecular Technologies, Kumamoto, Japan) according to the protocol. Cells were then seeded on 96-well plates (3×10^3 cells/well) and cultured for 12 h. For each well, 10 μl CCK-8 reagent were added at indicated time points. Then, the absorbance value was recorded at 450 nm with a microplate reader (BioTek, Thorold, ON, Canada) and cell. Each group was set with three replicate wells.

Table I. Primer sequences for RT-PCR.

Gene names	Primer sequences	Species
circ_0056618	Forward: 5'-GAACCCACCCCACCTCTAC-3' Reverse: 5'-CTTCCCCGGGATAAACAAACC-3'	Human
miR-206	Forward: 5'-CGGGCTTGTGGAATGGTAAGC-3' Reverse: 5'-GGGCATACATCGGCTAATACA-3'	Human
β-actin	Forward:5'-GCTTCGGCAGCACATATACTAAAAT-3' Reverse:5'-AGGGTACATGGTGGTGCCGCCA-3'	Human
U6	Forward:5'-CGCTTCACGAATTTGCGTGTC-3' Forward:5'-TAAAACGCAGCTCAGTAACAGTC-3'	Human

Tube Formation Assay

HT29 cells were seeded on 48-well plates (3×10^4 cells/well) and cells were coated with ice-cold Matrigel (Phenol Red-Free, BD Biosciences, Franklin Lakes, NJ, USA), which was then incubated at 37°C for 30 mins. Next, HT29 cells were harvested and suspended in 2% FBS-reduced medium. Moreover, cells were plated in Matrigel-coated wells with a density of 15×10^4 cells/well and incubated at 37°C for 30 min for cell attachment. Images of the tubular structures were photographed using a real-time cell recorder (NanoEntek, Seoul, South-Korea) after 12 h and the number of tube branches was counted.

Cell Migration Assay

Cell migration ability was measured by transwell assay, HT29 cells (2×10^4 cells/well) were seeded into the upper transwell chambers (BD Biosciences, Franklin Lakes, NJ, USA) with 10% FBS, and 20% FBS was added into the lower chambers. After culturing at 37°C with 5% CO_2 for 24 h, migrated cells on the other side were fixed with 95% methanol for 10 mins and stained with 0.5% crystal violet (Beyotime, Shanghai, China). Migrated cells were examined and counted using a light microscope (Olympus Corporation, Tokyo, Japan). Three independent experiments were repeated to get the mean value.

Luciferase Gene Reporter Assay

To examine the 3'-UTR Luciferase activity, the wild type and mutant sequences of circ_0056618, VEGF-A and CXCR4 were constructed into GLO plasmids (Promega, Madison, WI, USA). HT29 cells and 293 cells were respectively seeded in 48-well plates and cultured at an incubator for 12 h. Then, Renilla Luciferase vector and firefly Luciferase plasmids were transfected into cells for 12 h; then, indicated wild type and mutant sequences were respectively transfected into the prepared cells for 24 h. In addition, miR-206 mimic or mimic NC has respectively transfected these indicated cells for another 24 h. Finally, cells were harvested, and Luciferase activities were measured using a Luciferase assay system (Promega, Madison, WI, USA). Relative activities of Luciferase were calculated and normalized to the Renilla Luciferase activity.

Statistical Analysis

All data were analyzed by SPSS 18.0 (SPSS Inc., Chicago, IL, USA) and GraphPad Prism 6.0 (La Jolla, CA, USA). Count data were processed by chi-square test. Statistical significance was analyzed by Student's *t*-test or one-way ANOVA and SNK method. Correlations were analyzed using Pearson's correlation analysis and overall survival of patients was analyzed by Kaplan-Meier survival test. $p<0.05$ was considered to be statistically significant.

Results

Circ_0056618 Was Evaluated In CRC Tissues and CRC Cell Lines

For the first time, we detected the circ_0056618 expression by RT-PCR in 60 paired CRC tissues and non-tumor tissues. Results revealed that circ_0056618 was evaluated in CRC tissues, compared to non-tumor tissues (n=60) (Figure 1A) ($p<0.001$). Notably, we found that circ_0056618 in patients with metastasis (n=26) was much higher than that in patients without metastasis (n=34) (Figure 1B) ($p<0.001$). Besides, Kaplan-Meier survival analysis revealed that CRC patients with circ_0056618 high expression showed a lower overall survival (OS) than patients with circ_0056618 low expression (Figure 1C) ($p<0.05$). Additionally, we found that expressions of circ_0056618 in CRC cell lines were significantly increased (Figure 1D) ($p<0.05$). In addition, clinicopathological analyses showed that the high expression of circ_0056618 was associated with tumor size, TNM stage, lymph node metastasis and distant metastasis in CRC patients (Table I) ($p<0.05$). Collectively, these data suggested that circ_0056618 was increased in CRC tissues, which might play some roles in the development of CRC.

Circ_0056618 Inhibition Repressed Cell Proliferation, Migration and Angiogenesis In HT29 Cells

To investigate the functions of circ_0056618 in CRC, circ_0056618 si-RNA was constructed (si-circ_0056618), resulting with circ_0056618 downregulation (Figure 2A) ($p<0.001$). Then, CCK-8 assay revealed that circ_0056618 inhibition repressed cell proliferation, compared to control and si-NC (Figure 2B) ($p<0.01$). Furthermore, tube formation assay showed that circ_0056618 inhibition repressed cell capacity of angiogenesis, compared to control and si-NC (Figure 2C) ($p<0.01$). Moreover, transwell assay demonstrated that circ_0056618 inhibition repressed cell migration ability in HT29 cells (Figure 2D, E) ($p<0.01$).

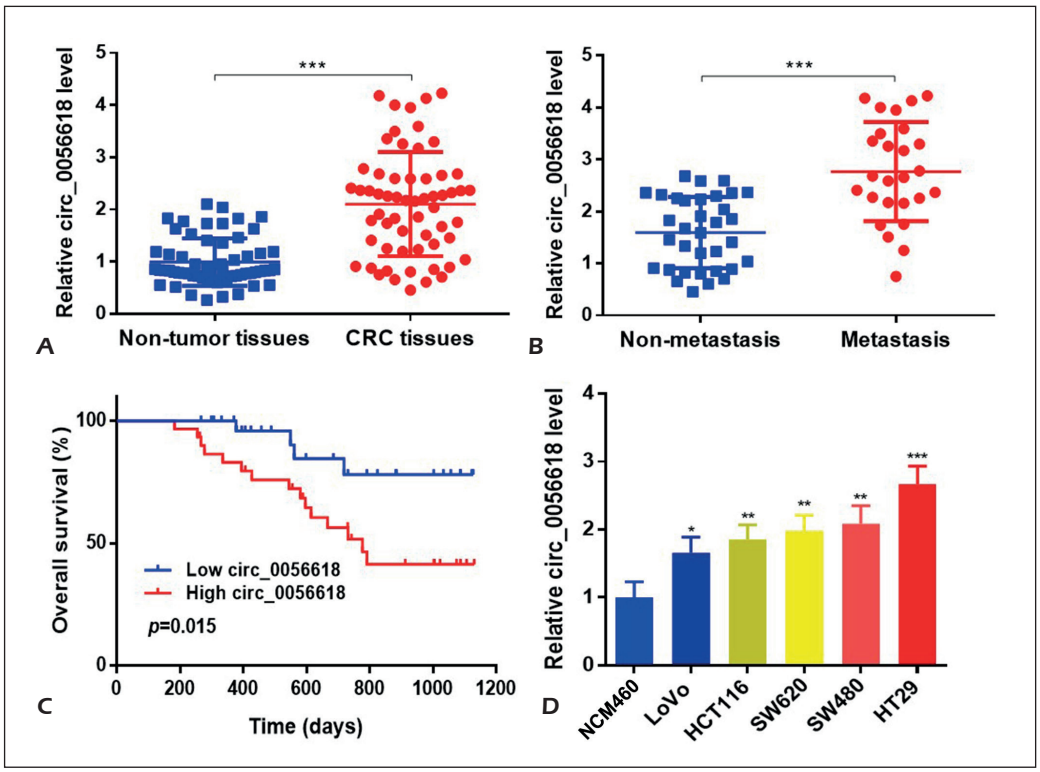

Figure 1. Circ_0056618 was evaluated in CRC tissues and CRC cell lines. **A**, RT-PCR was used to detect circ_0056618 levels in CRC tissues (n=60) and corresponding non-tumor tissues (n=60). **B**, Circ_0056618 levels in CRC patients with metastasis (n=26) and non-metastasis (n=34) were analyzed. **C**, Kaplan-Meier survival analysis was performed to analyze the OS for patients with circ_0056618 low and high expression. **D**, RT-PCR was used to detect circ_0056618 levels in CRC cell lines. *p<0.05, **p<0.01, ***p<0.001.

Additionally, Western blot (WB) was performed to detect protein expressions of proliferation associated gene Cyclin D1, migration associated genes, including N-cadherin and E-cadherin, angiogenesis associated gene VEGF-A. Results showed that protein levels of Cyclin D1, N-cadherin and VEGF-A were repressed, while E-cadherin was increased (Figure 2F, G) (p<0.01). These data suggested that circ_0056618 inhibition repressed cell proliferation, migration and angiogenesis in HT29 cells.

MiR-206 Was Reduced In CRC Tissues, Which Could Be Sponged With Circ_0056618 In HT29 Cells

To understand the mechanism that circ_0056618 regulated proliferation, migration and angiogenesis in CRC cells, bioinformatics analysis was used to predict target miRNAs of circ_0056618. Results showed that miR-206 might be a target for circ_0056618, which had been revealed to be related with the progression of cancers, including CRC[10-15]. Then, we detected miR-206 expressions in CRC tissue samples and the responding non-tumor tissues, which showed that miR-206 was reduced in CRC tissues (Figure 3A) (p<0.001), especially in patients with metastasis, compared to patients without metastasis (Figure 3B) (p<0.001). Correlation analysis showed that miR-206 was negatively correlated with circ_0056618 in metastasis patients (Figure 3C) (p<0.01), but not in non-metastasis patients (Figure 3D) (p>0.05). Moreover, we found that miR-206 levels were significantly reduced in CRC cell lines (Figure 3E) (p<0.01), while they were increased after si-circ_0056618 transfection (Figure 3F) (p<0.001). These data indicated that circ_0056618 was negatively related with miR-206, which might be a target for circ_0056618. To verify that circ_0056618 could competitively sponge with miR-206, wild type and mutant sequences of circ_0056618 were constructed into GLO vectors (Figure 3G) and Luciferase gene reporter assay was performed. Results revealed that the relative Luciferase activity in HT29 cells co-transfected with wt-circ_0056618 and miR-

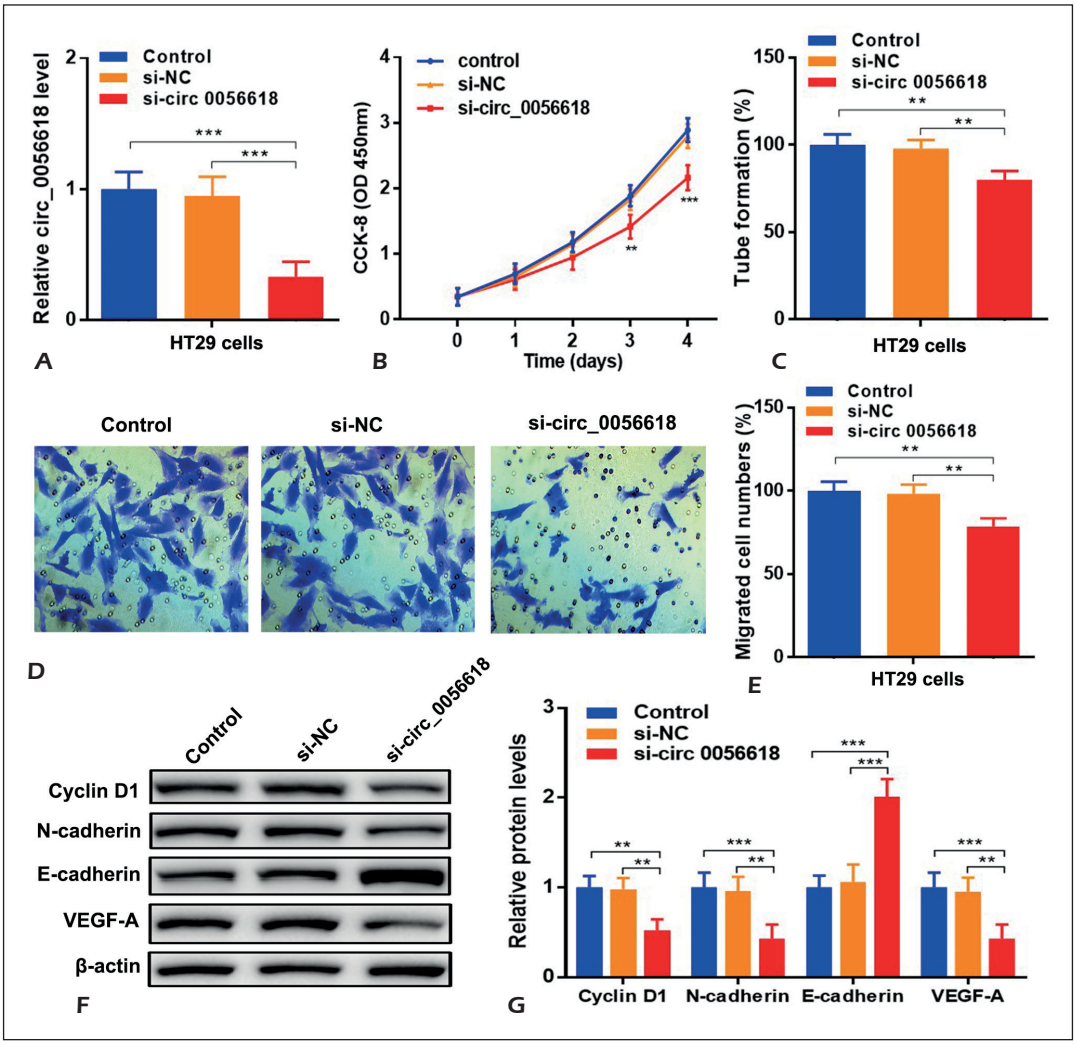

Figure 2. Circ_0056618 inhibition repressed cell proliferation, migration and angiogenesis in HT29 cells. Si-circ_0056618 or si-NC was transfected into HT29 cells. **A**, Circ_0056618 expressions were detected by RT-PCR. **B**, Proliferation abilities of treated cells were measured by CCK-8 assay. **C**, Tube formation assay was performed to detected angiogenesis ability of HT29 cells. **D**-**E**, Migration abilities were measured by transwell assay. **F**-**G**, Protein levels of Cyclin D1, N-cadherin, E-cadherin and VEGF-A were detected by WB (magnifications x 0.8). **p<0.01, ***p<0.001.

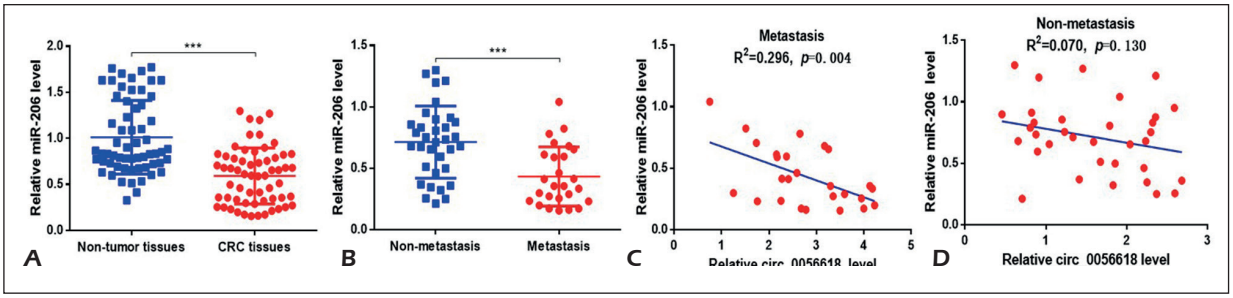

Figure 3. MiR-206 was reduced in CRC tissues, which could be sponged with circ_0056618 in HT29 cells. **A**, MiR-206 expressions were detected by RT-PCR in CRC tissues (n=60) and non-tumor tissues (n=60). **B**, MiR-206 levels in CRC patients with metastasis (n=26) and non-metastasis (n=34) were analyzed. **C**-**D**, Correlation analysis was performed between circ_0056618 and miR-206 in patients with metastasis and non-metastasis. **E**-**F**, MiR-206 expressions were detected in CRC cell lines and in HT29 cells after transfection with si-NC or si-circ_0056618. **G**, Wild type and mutant sequences of circ_0056618 were constructed into GLO vectors. H, Luciferase gene reporter assay was performed. *p<0.05, **p<0.01, ***p<0.001.

206 mimic was inhibited, while it was reversed following co-transfecting with mut-LINC00511 (Figure 3H) (p<0.01). These data indicated that miR-206 was reduced in CRC tissues, which could be sponged with circ_0056618 in HT29 cells.

MiR-206 Overexpression Repressed Cell Proliferation, Migration and Angiogenesis In HT29 Cells

To find out whether miR-206 could regulate the progression of CRC, miR-206 mimic was transfected into HT29 cells, which resulted with miR-206 overexpression (Figure 4A) (p<0.001). Then, CCK-8 assay revealed that miR-206 overexpression repressed cell proliferation (Figure 4B) (p<0.01). Furthermore, tube formation assay showed that miR-206 overexpression repressed cell capacity of angiogenesis (Figure 4C) (p<0.01). Besides, transwell assay demonstrated that miR-206 overexpression repressed cell migration ability in HT29 cells (Figure 4D, E) (p<0.01). In addition, WB results showed that the protein levels of Cyclin D1, N-cadherin and VEGF-A were inhibited, while E-cadherin was promoted (Figure 4F,

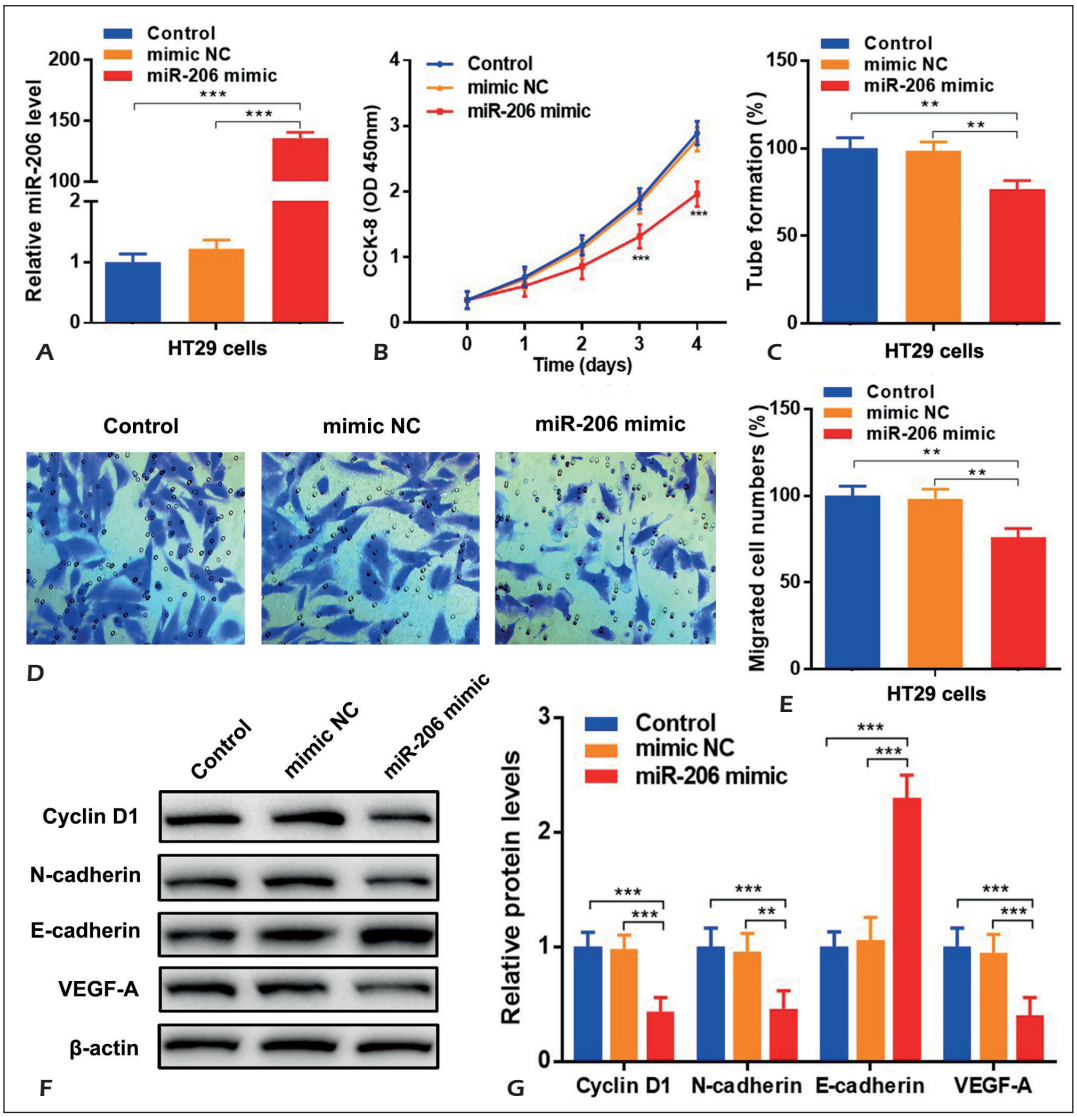

Figure 4. MiR-206 overexpression repressed cell proliferation, migration and angiogenesis in HT29 cells. MiR-206 mimic or mimic NC was transfected into HT29 cells. **A**, Circ_0056618 expressions were detected by RT-PCR. **B**, Cell Proliferation abilities were measured by CCK-8 assay. **C**, Tube formation assay was performed to detect cell angiogenesis ability. **D-E**, Migration abilities were measured by transwell assay. **F-G**, Protein levels of Cyclin D1, N-cadherin, E-cadherin and VEGF-A were detected by WB (magnifications x 0.8). **p<0.01, ***p<0.001.

G) (p<0.01). These data suggested that miR-206 played some roles in the development of CRC, which could repress cell proliferation, migration and angiogenesis in HT29 cells

MiR-206 Was Negatively Related With VEGF-A and CXCR4 In CRC Tissues

To further understand how miR-206 regulated the progression of CRC, we used Targetscan database to analyze the target genes of miR-206. It showed that VEGF-A and CXCR4 were predicted to be two potential targets for miR-206; further, these two genes had been reported to be closely associated with tumor formation and angiogenesis in cancers[34-36]. Therefore, we detected the protein levels of VEGF-A and CXCR4 in CRC tissues and non-tumor tissues. Results showed that both VEGF-A and CXCR4 were significantly elevated in CRC tissues (Figure 5A, B) (p<0.001), and the levels of VEGF-A and CXCR4 in patients with metastasis were much higher than that in patients without metastasis (Figure 5C, D) (p<0.001). Furthermore, correlation analysis indicated that VEGF-A and CXCR4 were both negatively related with miR-206 in metastasis patients (Figure 5E, F) (p<0.05), but not in non-metastasis patients (Figure 5G, H) (p>0.05). Additionally, we found that protein levels of VEGF-A and CXCR4 were upregulated in CRC cell lines (Figure 5I, J) (p<0.05), while levels of VEGF-A and CXCR4 were repressed after miR-206 mimic transfection into HT29 cells (Figure 5K, L) (p<0.001). Above all, these data suggested that miR-206 was negatively related with VEGF-A and CXCR4 in CRC tissues and HT29 cells.

MiR-206 Could Directly Bind With VEGF-A and CXCR4 In HT29 and 293 Cells

Above data suggested that miR-206 was negatively related with VEGF-A and CXCR4, which were predicted to be two potential target genes for miR-206 by Targetscan database. To verify that miR-206 could directly bind to VEGF-A and

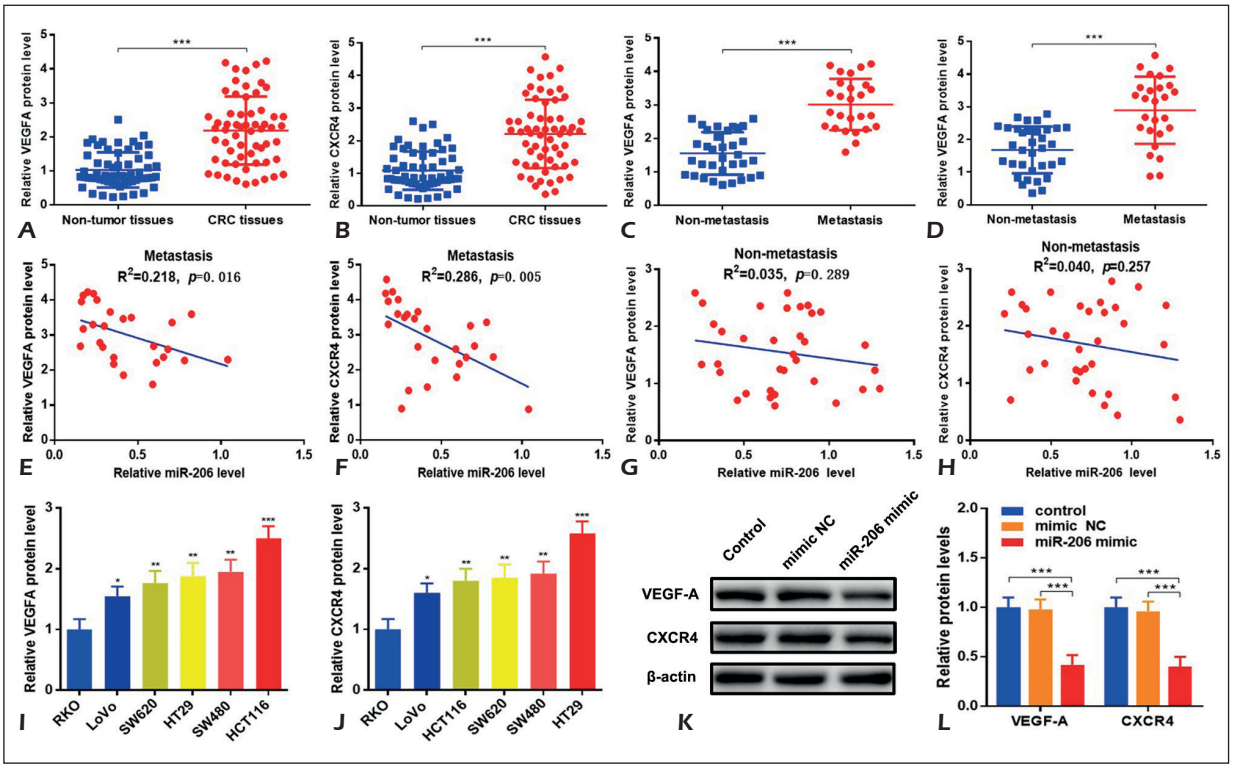

Figure 5. MiR-206 was negatively related with VEGF-A and CXCR4 in CRC tissues. **A-B**, Protein expressions of VEGF-A and CXCR4 were detected by WB in CRC tissues (n=60) and non-tumor tissues (n=60). **C-D**, Protein expressions of VEGF-A and CXCR4 were analyzed in CRC patients with metastasis (n=26) and non-metastasis (n=34). **E-H**, Correlation analysis was performed between miR-206 with VEGF-A and CXCR4 in patients with metastasis and non-metastasis. I, J, Protein levels of VEGF-A and CXCR4 were detected in CRC cell lines. K, L, Protein levels of VEGF-A and CXCR4 were detected in HT29 cells after transfection with mimic-NC or miR-206 mimic. *p<0.05, **p<0.01, ***p<0.001.

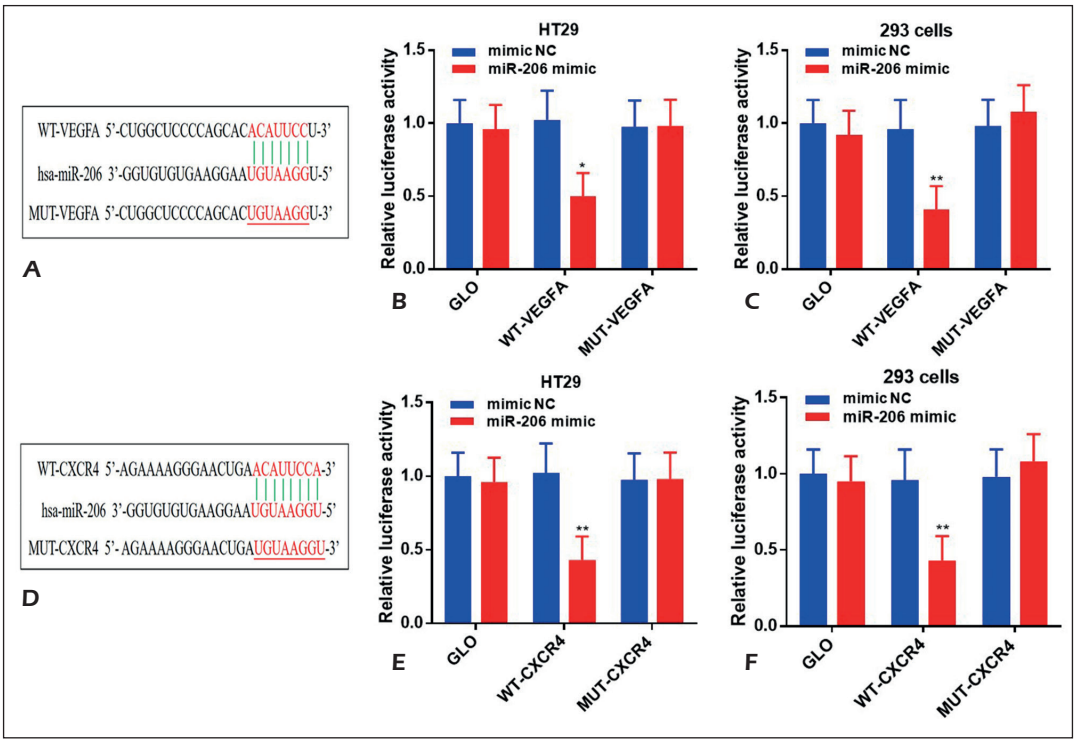

Figure 6. MiR-206 could directly bind with VEGF-A and CXCR4 in HT29 and 293 cells. **A-D**, Wild type and mutant sequences of VEGF-A or CXCR4 were constructed into GLO vectors. **B-C**, Luciferase gene reporter assay was performed to prove the binding site between miR-206 and VEGF-A in HT29 and 293 cells. **E-F**, Luciferase gene reporter assay was performed to prove the binding site between miR-206 and CXCR4 in HT29 and 293 cells. *p<0.05, **p<0.01.

CXCR4, the wild type and mutant sequences of VEGF-A and CXCR4 were synthesized and constructed into GLO vectors (Figure 6A, D) and Luciferase gene reporter assay was performed. Results illustrated that the relative Luciferase activity in HT29 cells or 293 cells that co-transfected with WT-VEGF-A and miR-206 mimic was repressed, while it was reversed in MUT-VEGF-A group (Figure 6B, C) (p<0.05). Furthermore, the relative Luciferase activity in HT29 cells or 293 cells that co-transfected with WT- CXCR4 and miR-206 mimic was repressed, while it was reversed in MUT-CXCR4 group (Figure 6E, F) (p<0.01). Collectively, these data demonstrated that miR-206 could directly bind with VEGF-A and CXCR4 in HT29 and 293 cells.

Circ_0056618 Promoted Cell Proliferation, migration and angiogenesis through sponging with miR-206 and upregulating CXCR4 and VEGF-A in HT29 cells

Above all, according to these data, we might assume that circ_0056618 could sponge with miR-206, which would remove the repressing effects of CXCR4 and VEGF-A, thereby promoting tumor progression of cell proliferation, migration and angiogenesis. To verify that, we transfected miR-206 inhibitor or inhibitor NC into HT29 cells with si-circ_0056618 or si-NC to observe the effects. Results showed that the repressed circ_0056618 in si-circ_0056618 was increased following with miR-206 inhibitor transfection (Figure 7A) (p<0.001), while the increased miR-206 in si-circ_0056618 was inhibited following with miR-206 inhibitor transfection (Figure 7A) (p<0.001). Furthermore, CCK-8 assay revealed that the repressed cell proliferation capacity in si-circ_0056618 was increased following with miR-206 inhibitor transfection (Figure 7B) (p<0.01). Besides, tube formation assay showed that the repressed angiogenesis in si-circ_0056618 was promoted following with miR-206 inhibitor transfection (Figure 7C) (p<0.01). In addition, transwell assay illustrated that the repressed migration in si-circ_0056618 was reversed following with miR-206 inhibitor transfection (Figure 7D, E) (p<0.01). Finally, WB results showed that the repressed protein levels of CXCR4, VEGF-A, Cyclin D1 and

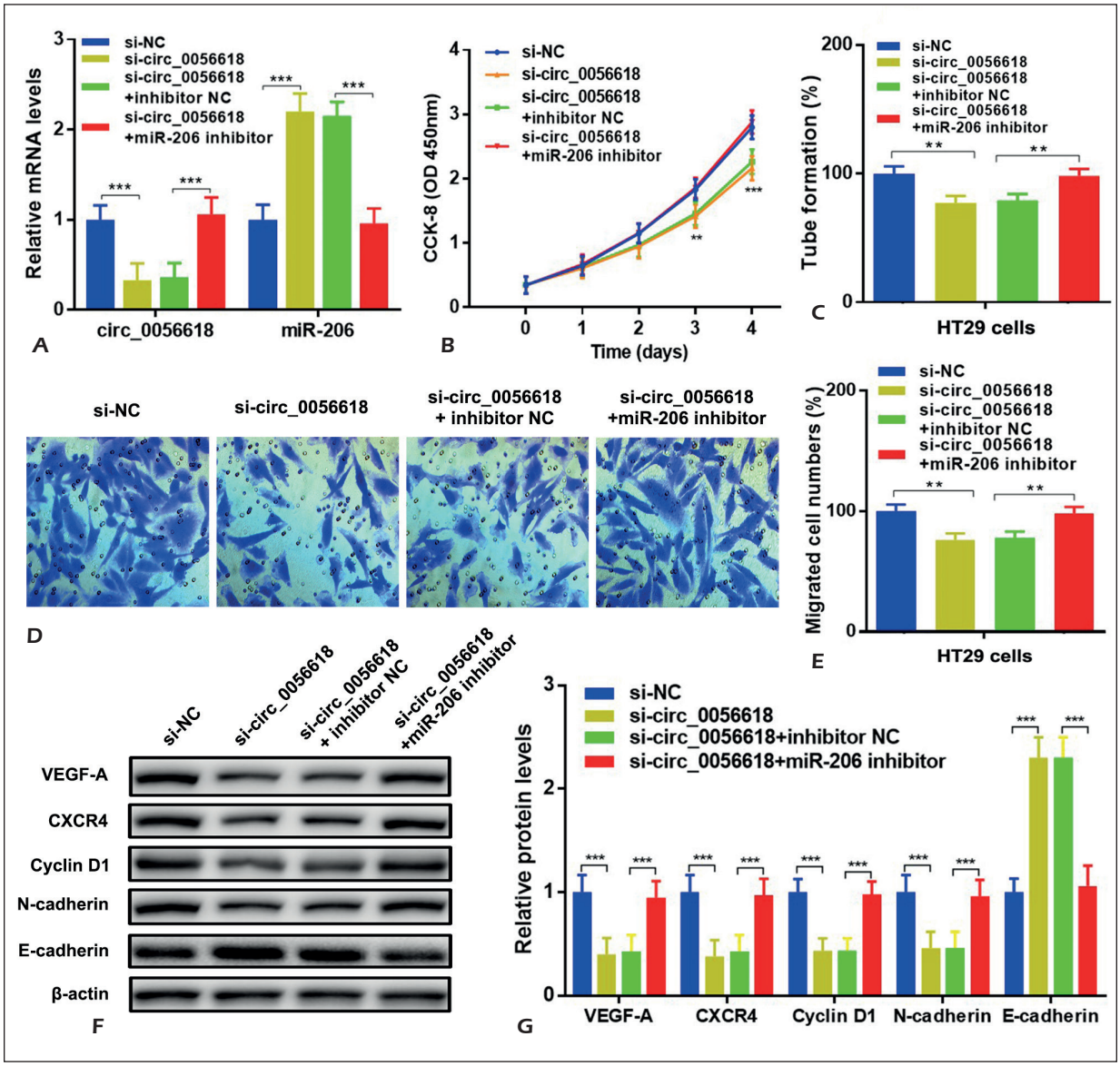

Figure 7. Circ_0056618 promoted cell proliferation, migration and angiogenesis through sponging with miR-206 and upregulating CXCR4 and VEGF-A in HT29 cells. MiR-206 inhibitor or inhibitor NC was transfected into HT29 cells with si-circ_0056618 or si-NC. **A**, The mRNA expressions of circ_0056618 and miR-206 were detected by RT-PCR. **B**, CCK-8 assay was used to measure cell proliferation abilities. **C**, Tube formation assay was performed to detect cell angiogenesis ability. **D-E**, Migration abilities were measured by transwell assay. **F-G**, Protein levels of CXCR4, VEGF-A, Cyclin D1, N-cadherin and E-cadherin were detected by WB (magnifications x 0.8). **p<0.01, ***p<0.001.

N-cadherin were increased, while the increased E-cadherin level in si-circ_0056618 was reduced following with miR-206 inhibitor transfection (Figure 7F, G) (p<0.001). Collectively, these results confirmed that Circ_0056618 promoted cell proliferation, migration and angiogenesis through sponging with miR-206 and upregulating CXCR4 and VEGF-A in CRC patients.

Discussion

CRC is a malignancy with high incidence and mortality for patients worldwide[1-4]. Although novel therapeutic treatments, chemotherapy and diagnosis methods have increased the 5-year survival rate for CRC patients; however, the outcome of patients with metastasis is extremely poor[1-4].

Therefore, novel biomarkers and treatments for CRC patients are needed to improve future prognosis for CRC patients. CircRNAs have been revealed to play important roles in CRC[10-15], which have the capacity to regulate biological functions through sponging with miRNA and affect its target gene expressions[16-20]. The expression of circ_0056618 in CRC was unknown. Then, we detected the circ_0056618 expressions in 60 paired tumor tissues and non-tumor tissues from CRC patients. Results revealed that circ_0056618 was evaluated in CRC tissues and CRC cell lines, which was associated with poor overall survival for CRC patients. Then, circ_0056618 might play some roles in CRC.

To investigate potential roles of circ_0056618 in CRC, si-circ_0056618 or si-NC was constructed into plasmids and transfected into HT29 cells, which resulted with circ_0056618 inhibition. We found that circ_0056618 inhibition reduced cell viability, tube formation and cell migration. Cyclin D1 is a protein that transits cells from G1 to S phase, which is responsible for cell proliferation in various cancers[37-39]. N-cadherin and E-cadherin are from cadherin family, N-cadherin helps to promote cell invasion and migration for cancers, while E-cadherin represses these functions[40,41]. VEGF-A and CXCR4 are two genes closely associated with tumor formation and angiogenesis in cancers[34-36]. WB results revealed that circ_0056618 inhibition repressed protein levels of Cyclin D1, VEGF-A, N-cadherin and promoted E-cadherin, which proved that circ_0056618 inhibition repressed cell proliferation, angiogenesis and migration. However, the mechanism remained unknown.

CircRNAs could affect biological functions through sponging with miRNAs and regulate target gene expressions[16-20]. We used bioinformatics analysis and miR-206 was predicted as a target miRNA, which was reported to regulate cell invasion, proliferation and angiogenesis in cancers[28-33]. We found that miR-206 was reduced in CRC patients and Luciferase reporter assay proved that circ_0056618 could directly bind to miR-206 in HT29 cells and miR-206 could regulate the biological functions of cell proliferation, angiogenesis and migration in CRC cell lines.

MiRNAs could affect various functions by binding to the 3'-UTR of target genes in diseases[24-27]. Therefore, target genes of miR-206 were analyzed using Targetscan database. VEGF-A and CXCR4 were predicted as potential target genes, which were related with the formation and angiogenesis of cancers[34-36]. We found that levels of VEGF-A and CXCR4 were upregulated in CRC tissues, which was negatively related with miR-206. Then, Luciferase reporter assay further confirmed that miR-206 could directly bind to VEGF-A and CXCR4 in HT29 cells and 293 cells, and regulate the progression of CRC. Finally, miR-206 inhibitor was transfected into HT29 cells with circ_0056618 inhibition. Results indicated that the repressed proliferation, migration and angiogenesis were ameliorated, which suggested that circ_0056618 regulated the tumor progression through sponging with miR-206 and affecting the expressions of VEGF-A and CXCR4 in CRC patients.

For the first time, we revealed that circ_0056618 was upregulated in human CRC tissues, which might be a prognostic marker for CRC. We demonstrated that circ_0056618 could promote cell proliferation of CRC; importantly, we found that circ_0056618 could interact with miR-206 and affect the expressions of VEGF-A and CXCR4, which were critical factors for cell migration and angiogenesis, thereby weakening cell migration ability. We uncovered a new molecule that might predict the prognosis and solve the difficult problem for CRC patients with metastasis. It might provide a new insight for the treatment of CRC and reducing the metastatic ability.

Conclusions

In all, we firstly revealed that circ_0056618 was increased in CRC tissues, which was related with the poor OS of CRC patients. We found that circ_0056618 could promote cell proliferation, migration and angiogenesis through sponging with miR-206 and upregulating CXCR4 and VEGF-A in CRC, which might provide a novel potential therapeutic target for treating CRC.

Conflict of Interests

The authors declare that they have no conflict of interests.

References

1) Chen W. Cancer statistics: updated cancer burden in China. Chin J Cancer Res 2015; 27: 1.
2) Chen W, Zheng R, Baade PD, Zhang S, Zeng H, Bray F, Jemal A, Yu XQ, He J. Cancer statistics in China, 2015. CA Cancer J Clin 2016; 66: 115-132.

3) Siegel RL, Miller KD, Jemal A. Cancer statistics, 2019. CA Cancer J Clin 2019; 69: 7-34.
4) Siegel RL, Miller KD, Fedewa SA, Ahnen DJ, Meester RGS, Barzi A, Jemal A. Colorectal cancer statistics, 2017. CA Cancer J Clin 2017; 67: 177-193.
5) Luo B, Tang CM, Chen JS. CircRNA and gastrointestinal cancer. J Cell Biochem 2019 Apr 4. doi: 10.1002/jcb.28610. [Epub ahead of print]
6) Yin Y, Long J, He Q, Li Y, Liao Y, He P, Zhu W. Emerging roles of circRNA in formation and progression of cancer. J Cancer 2019; 10: 5015-5021.
7) Feng J, Chen K, Dong X, Xu X, Jin Y, Zhang X, Chen W, Han Y, Shao L, Gao Y, He C. Genome-wide identification of cancer-specific alternative splicing in circRNA. Mol Cancer 2019; 18: 35.
8) Yang SJ, Wang DD, Zhou SY, Zhang Q, Wang JY, Zhong SL, Zhang HD, Wang XY, Xia X, Chen W, Yang SY, Hu JH, Zhao JH, Tang JH. Identification of circRNA-miRNA networks for exploring an underlying prognosis strategy for breast cancer. Epigenomics 2020; 12: 101-125.
9) Yu X, Ding H, Yang L, Yu Y, Zhou J, Yan Z, Guo J. Reduced expression of circRNA hsa_circ_0067582 in human gastric cancer and its potential diagnostic values. J Clin Lab Anal 2019 Nov 12:e23080. doi: 10.1002/jcla.23080. [Epub ahead of print]
10) Li H, Jin X, Liu B, Zhang P, Chen W, Li Q. CircRNA CBL.11 suppresses cell proliferation by sponging miR-6778-5p in colorectal cancer. BMC Cancer 2019; 19: 826.
11) Tian J, Xi X, Wang J, Yu J, Huang Q, Ma R, Zhang X, Li H, Wang L. CircRNA hsa_circ_0004585 as a potential biomarker for colorectal cancer. Cancer Manag Res 2019; 11: 5413-5423.
12) Li R, Wu B, Xia J, Ye L, Yang X. Circular RNA hsa_circRNA_102958 promotes tumorigenesis of colorectal cancer via miR-585/CDC25B axis. Cancer Manag Res 2019; 11: 6887-6893.
13) Wang X, Zhang H, Yang H, Bai M, Ning T, Deng T, Liu R, Fan Q, Zhu K, Li J, Zhan Y, Ying G, Ba Y. Exosome-delivered circRNA promotes glycolysis to induce chemoresistance through the miR-122-PKM2 axis in colorectal cancer. Mol Oncol 2020; 14: 539-555.
14) Liu K, Guo Y, Zheng K, Zou C, Wu H, Wang S, Ou L, Wang Y, Huang B, Wang X. Identification of the circRNA-miRNA-mRNA regulatory network of Hsp90 inhibitor-induced cell death in colorectal cancer by integrated analysis. Gene 2020; 727: 144232.
15) Li XN, Wang ZJ, Ye CX, Zhao BC, Li ZL, Yang Y. RNA sequencing reveals the expression profiles of circRNA and indicates that circDDX17 acts as a tumor suppressor in colorectal cancer. J Exp Clin Cancer Res 2018; 37: 325.
16) Wilusz JE. A 360 degrees view of circular RNAs: From biogenesis to functions. Wiley Interdiscip Rev RNA 2018; 9: e1478.
17) Memczak S, Jens M, Elefsinioti A, Torti F, Krueger J, Rybak A, Maier L, Mackowiak SD, Gregersen LH, Munschauer M, Loewer A, Ziebold U, Landthaler M, Kocks C, le Noble F, Rajewsky N. Circular RNAs are a large class of animal RNAs with regulatory potency. Nature 2013; 495: 333-338.
18) Li J, Yang J, Zhou P, Le Y, Zhou C, Wang S, Xu D, Lin HK, Gong Z. Circular RNAs in cancer: novel insights into origins, properties, functions and implications. Am J Cancer Res 2015; 5: 472-480.
19) Lasda E, Parker R. Circular RNAs: diversity of form and function. RNA 2014; 20: 1829-1842.
20) Zhang F, Zhang R, Zhang X, Wu Y, Li X, Zhang S, Hou W, Ding Y, Tian J, Sun L, Kong X. Comprehensive analysis of circRNA expression pattern and circRNA-miRNA-mRNA network in the pathogenesis of atherosclerosis in rabbits. Aging (Albany NY) 2018; 10: 2266-2283.
21) Labernadie A, Kato T, Brugués A, Serra-Picamal X, Derzsi S, Arwert E, Weston A, González-Tarragó V, Elosegui-Artola A, Albertazzi L, Alcaraz J, Roca-Cusachs P, Sahai E, Trepat X. A mechanically active heterotypic E-cadherin/N-cadherin adhesion enables fibroblasts to drive cancer cell invasion. Nat Cell Biol 2017; 19: 224-237.
22) Yan Z, Xiao Y, Chen Y, Luo G. Screening and identification of epithelial-to-mesenchymal transition-related circRNA and miRNA in prostate cancer. Pathol Res Pract 2020; 216: 152784.
23) Li H, Yao G, Feng B, Lu X, Fan Y. Circ_0056618 and CXCR4 act as competing endogenous in gastric cancer by regulating miR-206. J Cell Biochem 2018; 119: 9543-9551.
24) Bartel DP. MicroRNAs: target recognition and regulatory functions. Cell 2009; 136: 215-233.
25) Fang C, Li Y. Prospective applications of microRNAs in oral cancer. Oncol Lett 2019; 18: 3974-3984.
26) Qiao J, Du Y, Yu J, Guo J. MicroRNAs as potential biomarkers of insecticide exposure: a review. Chem Res Toxicol 2019; 32: 2169-2181.
27) Rahman MM, Brane AC, Tollefsbol TO. MicroRNAs and epigenetics strategies to reverse breast cancer. Cells 2019; 8. pii: E1214.
28) Zhu H, He G, Wang Y, Hu Y, Zhang Z, Qian X, Wang Y. Long intergenic noncoding RNA 00707 promotes colorectal cancer cell proliferation and metastasis by sponging miR-206. Onco Targets Ther 2019; 12: 4331-4340.
29) Dai C, Xie Y, Zhuang X, Yuan Z. MiR-206 inhibits epithelial ovarian cancer cells growth and invasion via blocking c-Met/AKT/mTOR signaling pathway. Biomed Pharmacother 2018; 104: 763-770.
30) Wang Y, Xu H, Si L, Li Q, Zhu X, Yu T, Gang X. MiR-206 inhibits proliferation and migration of prostate cancer cells by targeting CXCL11. Prostate 2018; 78: 479-490.
31) Wang P, Gu J, Wang K, Shang J, Wang W. MiR-206 inhibits thyroid cancer proliferation and invasion by targeting RAP1B. J Cell Biochem 2019; 120: 18927-18936.
32) Zhou Y, Wang M, Tong Y, Liu X, Zhang L, Dong D, Shao J, Zhou Y. MiR-206 promotes cancer progression by targeting full-length neurokinin-1 receptor in breast cancer. Technol Cancer Res Treat 2019; 18: 1078142816.
33) Jia KG, Feng G, Tong YS, Tao GZ, Xu L. MiR-206 regulates non-small cell lung cancer cell aerobic glycolysis by targeting hexokinase 2. J Biochem 2019 Nov 19. pii: mvz099. doi: 10.1093/jb/mvz099. [Epub ahead of print].

34) de Nigris F, Crudele V, Giovane A, Casamassimi A, Giordano A, Garban HJ, Cacciatore F, Pentimalli F, Marquez-Garban DC, Petrillo A, Cito L, Sommese L, Fiore A, Petrillo M, Siani A, Barbieri A, Arra C, Rengo F, Hayashi T, Al-Omran M, Ignarro LJ, Napoli C. CXCR4/YY1 inhibition impairs VEGF network and angiogenesis during malignancy. Proc Natl Acad Sci U S A 2010; 107: 14484-14489.
35) Fang Y, Sun B, Wang J, Wang Y. MiR-622 inhibits angiogenesis by suppressing the CXCR4-VEGFA axis in colorectal cancer. Gene 2019; 699: 37-42.
36) Zhong J, Li J, Wei J, Huang D, Huo L, Zhao C, Lin Y, Chen W, Wei Y. Plumbagin restrains hepatocellular carcinoma angiogenesis by Stromal Cell-Derived Factor (SDF-1)/CXCR4-CXCR7 axis. Med Sci Monit 2019; 25: 6110-6119.
37) Holah NS, Hemida AS. Cyclin D1 and PSA act as good prognostic and clinicopathological indicators for breast cancer. J Immunoassay Immunochem 2020; 41: 28-44.
38) Ramos-García P, González-Moles MÁ, González-Ruiz L, Ayén Á, Ruiz-Ávila I, Bravo M, Gil-Montoya JA. Clinicopathological significance of tumor cyclin D1 expression in oral cancer. Arch Oral Biol 2019; 99: 177-182.
39) Zhong Q, Hu Z, Li Q, Yi T, Li J, Yang H. Cyclin D1 silencing impairs DNA double strand break repair, sensitizes BRCA1 wildtype ovarian cancer cells to olaparib. Gynecol Oncol 2019; 152: 157-165.
40) Cao ZQ, Wang Z, Leng P. Aberrant N-cadherin expression in cancer. Biomed Pharmacother 2019; 118: 109320.
41) Labernadie A, Kato T, Brugués A, Serra-Picamal X, Derzsi S, Arwert E, Weston A, González-Tarragó V, Elosegui-Artola A, Albertazzi L, Alcaraz J, Roca-Cusachs P, Sahai E, Trepat X. A mechanically active heterotypic E-cadherin/N-cadherin adhesion enables fibroblasts to drive cancer cell invasion. Nat Cell Biol 2017; 19: 224-237.